Noname manuscript No.
(will be inserted by the editor)

Transverse oscillations of coronal loops

Michael S. Ruderman · Robert Erdélyi

Received: date / Accepted: date

Abstract On 14 July 1998 TRACE observed transverse oscillations of a coronal loop generated by an external disturbance most probable caused by a solar flare. These oscillations were interpreted as standing fast kink waves in a magnetic flux tube. Firstly, in this review we embark on the discussion of the theory of waves and oscillations in a homogeneous straight magnetic cylinder with the particular emphasis on fast kink waves. Next, we consider the effects of stratification, loop expansion, loop curvature, non-circular cross-section, loop shape and magnetic twist.

An important property of observed transverse coronal loop oscillations is their fast damping. We briefly review the different mechanisms suggested for explaining the rapid damping phenomenon. After that we concentrate on damping due to resonant absorption. We describe the latest analytical results obtained with the use of thin transitional layer approximation, and then compare these results with numerical findings obtained for arbitrary density variation inside the flux tube.

Very often collective oscillations of an array of coronal magnetic loops are observed. It is natural to start studying this phenomenon from the system of two coronal loops. We describe very recent analytical and numerical results of studying collective oscillations of two parallel homogeneous coronal loops.

The implication of the theoretical results for coronal seismology is briefly discussed. We describe the estimates of magnetic field magnitude obtained from the observed fundamental frequency of oscillations, and the estimates of the coronal scale height obtained using the simultaneous observations of the fundamental frequency and the frequency of the first overtone of kink oscillations.

In the last part of the review we summarise the most outstanding and acute problems in the theory of the coronal loop transverse oscillations.

Keywords Sun · Corona · Oscillations · Magnetohydrodynamics

M. S. Ruderman and R. Erdélyi
Solar Physics and Space Plasma Research Centre (SP^{2}RC), Department of Applied Mathematics, University of Sheffield, Hicks Building, Hounsfield Road, Sheffield, S3 7RH, United Kingdom
Tel.: +44-114-2223717
Fax: +114-114-2223809
E-mail: M.S.Ruderman@sheffield.ac.uk

1 Introduction

On 14 July 1998 TRACE observed a spectacular phenomenon in the solar corona. A coronal magnetic loop started to oscillate in the transverse direction after having been hit by a disturbance most probably caused by a solar flare. This observation was reported by Aschwanden et al. (1999) and Nakariakov et al. (1999), and interpreted as standing fast kink wave in a magnetic flux tube. It was also pointed out by Nakariakov et al. (1999) that the oscillation was strongly damped with the characteristic damping time of a few oscillation periods. Later, similar observations were reported by, e.g., Schrijver and Brown (2000); Aschwanden et al. (2002); Schrijver et al. (2002); Aschwanden (2006).

After this first observation the transverse oscillations of coronal loops received ample attention from theorists. In the first theoretical studies the simplest model of a coronal magnetic loop was used. In this model a coronal loop is represented by a straight homogeneous magnetic cylinder with the magnetic field lines frozen in the dense photospheric plasma at the foot points. Then more sophisticated models were developed. These models take into account such effects as the density variation along and across the loop, the loop curvature, the loop non-circular cross-section, the variation of the loop radius along the loop, and the twist of the magnetic field lines.

In spite of great progress made in the theoretical study of transverse coronal loop oscillations, there are still many outstanding problems in this area of solar physics. In this review we describe the state-of-the art in the theory of transverse coronal loop oscillations and discuss problems that should be solved to make the theory more complete and applicable to the reality. The paper is organised as follows. In the next section we briefly outline the theory of waves in straight homogeneous magnetic tubes. In Sect. 3 we describe the method of studying transverse coronal loop oscillations based on the use of asymptotic expansions. In Sect. 4 we consider the effect of variation of the density and loop radius along the loop. In Sect. 5 we study kink oscillations of twisted magnetic tubes. In Sect. 6 we briefly discuss the effect of the loop curvature. In Sect. 7 we consider kink oscillations of loops with the elliptic cross-sections. In Sect. 8 we study the kink oscillations of a magnetic tube that consists of a core cylinder surrounded with a cylindrical annulus, the plasma densities being different in the cylinder and annulus. In Sect. 9 we consider the collective oscillations of two straight homogeneous parallel coronal loops. In Sect. 10 we describe the damping mechanisms of kink oscillations. In Sect. 11 the application of the theory of kink oscillations to coronal seismology is reviewed. Finally, in Sect. 12 we conclude and discuss outstanding problems in the theory of coronal loop transverse oscillations. In this review we do not consider the excitation mechanisms of the coronal loop transverse oscillations. These mechanisms are described in the review by Terradas (2009) in this issue.

2 Eigenmodes of straight homogeneous magnetic tubes

The eigenmodes of straight homogeneous magnetic tubes have been studied by many authors. One of the most complete investigations of these eigenmodes is given in Edwin and Roberts (1983) (see also the review papers by Aschwanden (2006); Roberts and Nakariakov (2003); Nakariakov and Verwichte (2005); Erdélyi (2008)). In this section we give a very brief review of the properties of these eigenmodes. The starting point

of our analysis is the linearised system of ideal MHD equations,

$$\rho = -\nabla \cdot (\rho_0 \boldsymbol{\xi}), \tag{1}$$

$$\rho_0 \frac{\partial^2 \boldsymbol{\xi}}{\partial t^2} = -\nabla P + \frac{1}{\mu_0}(\boldsymbol{B}_0 \cdot \nabla)\boldsymbol{b} + \frac{1}{\mu_0}(\boldsymbol{b} \cdot \nabla)\boldsymbol{B}_0, \tag{2}$$

$$\boldsymbol{b} = \nabla \times (\boldsymbol{\xi} \times \boldsymbol{B}_0), \tag{3}$$

$$p - C_S^2 \rho = \boldsymbol{\xi} \cdot (C_S^2 \nabla \rho_0 - \nabla p_0). \tag{4}$$

Here ρ_0, p_0 and $\boldsymbol{B}_0$ are the background density, plasma pressure and magnetic field. The background state is assumed to be static, so that all the background quantities are independent of time, and the background velocity is zero. The quantities ρ, p and $\boldsymbol{b}$ are the perturbations of the density, plasma pressure and magnetic field; $\boldsymbol{\xi}$ is the plasma displacement; $P = p + \boldsymbol{B}_0 \cdot \boldsymbol{b}/\mu_0$ is the perturbation of the total pressure (plasma plus magnetic); μ_0 is the magnetic permeability of empty space and $C_S^2 = \gamma p_0/\rho_0$ is the square of the sound speed, γ being the ratio of specific heats.

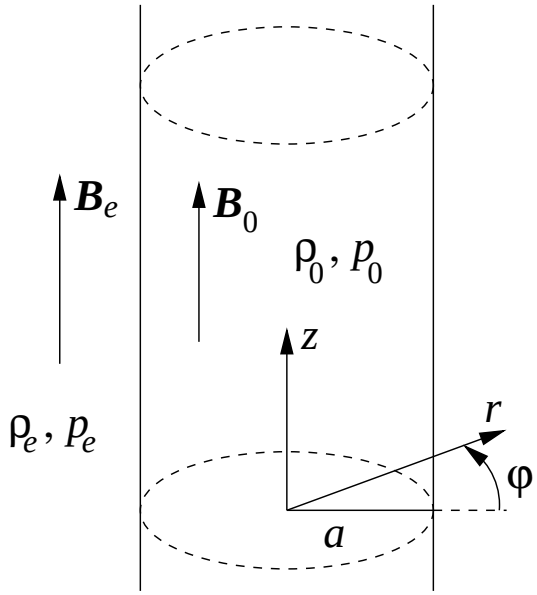

Fig. 1 The background state consisting of an infinite magnetic tube.

In what follows we consider the background state in the form of an infinite magnetic tube (see Fig. 1). In this background state all the background quantities are constant inside and outside the infinite cylinder of radius a, while, in general, they have jumps across the cylinder boundary. The magnetic field is parallel to the cylinder axis. In what follows we retain the subscript '0' for the background quantities inside the cylinder, while we use the subscript 'e' to indicate the background quantities in the surrounding plasma. The total background pressure has to be continuous at the tube boundary,

$$p_0 + \frac{B_0^2}{2\mu_0} = p_e + \frac{B_e^2}{2\mu_0}. \tag{5}$$

In our analysis we use cylindrical coordinates r, φ, z and introduce the corresponding components of the displacement and magnetic field perturbation, $\boldsymbol{\xi} = (\xi_r, \xi_\varphi, \xi_z)$ and $\boldsymbol{b} = (b_r, b_\varphi, b_z)$.

In what follows we consider only trapped waves and neglect leaky waves. This means that the perturbations have to decay far from the cylinder, i.e. when $r \to \infty$. At the cylinder boundary the normal component of the displacement and the perturbation of the total pressure have to be continuous,

$$\xi_{r0} = \xi_{re}, \quad P_0 = P_e. \tag{6}$$

It is straightforward to transform the system of Eqs. (1)-(4) to the form

$$\frac{\partial^4 P}{\partial t^4} - \left(C_S^2 + V_A^2\right)\nabla^2 \frac{\partial^2 P}{\partial t^2} + C_S^2 V_A^2 \nabla^2 \frac{\partial^2 P}{\partial z^2} = 0, \tag{7}$$

$$\frac{\partial^2 \xi_r}{\partial t^2} - V_A^2 \frac{\partial^2 \xi_r}{\partial z^2} = -\frac{1}{\rho_0}\frac{\partial P}{\partial r}, \tag{8}$$

$$\frac{\partial^2 \xi_\varphi}{\partial t^2} - V_A^2 \frac{\partial^2 \xi_\varphi}{\partial z^2} = -\frac{1}{r\rho_0}\frac{\partial P}{\partial \varphi}, \tag{9}$$

$$\frac{\partial^2 \xi_z}{\partial t^2} - C_T^2 \frac{\partial^2 \xi_z}{\partial z^2} = -\frac{C_T^2}{\rho_0 V_A^2}\frac{\partial P}{\partial z}, \tag{10}$$

$$b_r = B_0 \frac{\partial \xi_r}{\partial z}, \quad b_\varphi = B_0 \frac{\partial \xi_\varphi}{\partial z}, \quad b_z = -\frac{B_0}{r}\left(\frac{\partial (r\xi_r)}{\partial r} + \frac{\partial \xi_\varphi}{\partial \varphi}\right), \tag{11}$$

$$\rho = -\rho_0 \left(\frac{1}{r}\frac{\partial (r\xi_r)}{\partial r} + \frac{1}{r}\frac{\partial \xi_\varphi}{\partial \varphi} + \frac{\partial \xi_z}{\partial z}\right), \quad p = C_S^2 \rho, \tag{12}$$

where the squares of the Alfvén and tube speeds are given by

$$V_A^2 = \frac{B_0^2}{\mu_0 \rho_0}, \quad C_T^2 = \frac{C_S^2 V_A^2}{C_S^2 + V_A^2}, \tag{13}$$

and ∇^2 is the Laplacian given in cylindrical coordinates by

$$\nabla^2 = \frac{1}{r}\frac{\partial}{\partial r} r \frac{\partial}{\partial r} + \frac{1}{r^2}\frac{\partial^2}{\partial \varphi^2} + \frac{\partial^2}{\partial z^2}. \tag{14}$$

Now we Fourier-analyse the perturbations of all quantities and look for solutions in the form of eigenmodes. This means that we take all dependent variables in Eqs. (7)-(12) proportional to $\exp[i(-\omega t + m\varphi + kz)]$, where m is integer. Then the system of Eqs. (7)-(12) reduces to

$$\frac{d^2 P}{dr^2} + \frac{1}{r}\frac{dP}{dr} - \left(\Lambda^2 + \frac{m^2}{r^2}\right) P = 0, \tag{15}$$

$$(\omega^2 - V_A^2 k^2)\xi_r = \frac{1}{\rho_0}\frac{dP}{dr}, \tag{16}$$

$$(\omega^2 - V_A^2 k^2)\xi_\varphi = \frac{imP}{r\rho_0}, \tag{17}$$

$$(\omega^2 - C_T^2 k^2)\xi_z = \frac{iC_T^2 kP}{\rho_0 V_A^2}, \tag{18}$$

$$b_r = iB_0 k\xi_r, \quad b_\varphi = iB_0 k\xi_\varphi, \quad b_z = -\frac{B_0}{r}\left(\frac{d(r\xi_r)}{dr} + im\xi_\varphi\right), \tag{19}$$

$$\rho = -\rho_0\left(\frac{1}{r}\frac{d(r\xi_r)}{dr} + \frac{im}{r}\xi_\varphi + ik\xi_z\right), \quad p = C_S^2\rho, \tag{20}$$

where

$$\Lambda^2 = \frac{(C_S^2k^2 - \omega^2)(V_A^2k^2 - \omega^2)}{(C_S^2 + V_A^2)(C_T^2k^2 - \omega^2)}. \tag{21}$$

When $m = 0$, there is one special solution to the system of Eqs. (15)-(20). In this solution, inside the cylinder, only ξ_φ and b_φ are non-zero, while $\xi_r = \xi_z = b_r = b_z = P = \rho = p = 0$; ξ_φ is an arbitrary function of r, and $b_\varphi = iB_0k\xi_\varphi$. The external plasma is not perturbed. It is straightforward to see that the boundary conditions (6) are satisfied automatically. This solution describes the *torsional Alfvén* wave. Recently the observation of this wave was reported by Jess et al. (2009). It follows from Eq. (17) that the phase speed of this wave is equal to V_{A0}. This is the only solution to Eqs. (15)-(20) with $\omega^2 = V_{A0}^2k^2$. We also can consider a similar solution that describes perturbations in the external plasma, while the plasma inside the cylinder is not perturbed. It describes the torsional Alfvén wave with the phase speed equal to V_{Ae}. This is the only solution to Eqs. (15)-(20) with $\omega^2 = V_{Ae}^2k^2$.

Now we assume that $\omega^2 \neq V_{A0,e}^2k^2$. The restriction that we only consider trapped waves, i.e. waves evanescent in the external plasma, is equivalent to $\Lambda_e^2 > 0$. It follows from the condition $\omega^2 \neq V_{A0,e}^2k^2$ that there are no non-trivial solutions to Eqs. (15)-(20) with $P = 0$. Equation (15) is the modified Bessel equation. Its solution vanishing as $r \to \infty$ is given by $P_e = A_eK_m(\Lambda_e r)$, where K_m is the modified Bessel function of the second kind (McDonald function), and A_e is an arbitrary constant. The solution of Eq. (15), regular at $r = 0$, is $P_0 = A_0I_m(\Lambda_0 r)$, where I_m is the modified Bessel function of the first kind, and A_0 is an arbitrary constant.

While $\Lambda_e^2 > 0$, Λ_0^2 can have any sign. A wave mode is called a *surface wave* when $\Lambda_0^2 > 0$, and a *body wave* when $\Lambda_0^2 < 0$ (see, e.g., Roberts (1981)). In the latter case $\Lambda_0 = i|\Lambda_0|$ and $I_m(\Lambda_0 r) = i^m J_m(|\Lambda_0|r)$, where J_m is the Bessel function.

It follows from Eqs. (16) that

$$\xi_{r0} = \frac{A_0\Lambda_0 I_m'(\Lambda_0 r)}{\rho_0(\omega^2 - V_{A0}^2k^2)}, \quad \xi_{re} = \frac{A_e\Lambda_e K_m'(\Lambda_e r)}{\rho_e(\omega^2 - V_{Ae}^2k^2)},$$

where the prime indicates the derivative. Substituting the expressions for $P_{0,e}$ and $\xi_{0,e}$ in the boundary conditions (6) we obtain a system of two linear homogeneous algebraic equations for A_0 and A_e. This system possesses a non-trivial solution only when its determinant is equal to zero. This condition gives the dispersion equation determining the dependence of ω on k,

$$\rho_0(V_{A0}^2k^2 - \omega^2)\Lambda_e\frac{K_m'(\Lambda_e a)}{K_m(\Lambda_e a)} = \rho_e(V_{Ae}^2k^2 - \omega^2)\Lambda_0\frac{I_m'(\Lambda_0 a)}{I_m(\Lambda_0 a)}. \tag{22}$$

This equation is valid both when $\Lambda_0^2 > 0$ as well as when $\Lambda_0^2 < 0$. However, in the latter case we have to deal with complex quantities. To avoid this it is better to transform Eq. (22) to

$$\rho_0(V_{A0}^2k^2 - \omega^2)\Lambda_e\frac{K_m'(\Lambda_e a)}{K_m(\Lambda_e a)} = \rho_e(V_{Ae}^2k^2 - \omega^2)|\Lambda_0|\frac{J_m'(|\Lambda_0|a)}{J_m(|\Lambda_0|a)}. \tag{23}$$

The properties of the dispersion equations (22) and (23) depend very much on the relations between the quantities V_{A0}, C_{S0}, V_{Ae} and C_{Se}. Since we are mainly interested in waves in the corona, we consider the relations typical for the coronal conditions. The corona is strongly dominated by the magnetic field. The plasma pressure in the corona is much smaller than the magnetic pressure. Then it follows from Eq. (5) that $B_0 \approx B_e$. The plasma density inside coronal magnetic loops is larger than that in the surrounding plasma. As a result we obtain that $V_{A0} < V_{Ae}$. The typical values of the sound and Alfvén speed in the corona are 100 km/s and 1000 km/s respectively, so that $C_{S0,e} \ll V_{A0}$.

A comprehensive study of waves in a magnetic tube under coronal conditions can be found in Edwin and Roberts (1983). Here we only present the main results of this study. In what follows we concentrate on sausage waves ($m = 0$) and kink waves ($m = 1$). The dispersion curves showing the dependence of the phase speed of wave modes on the wavenumber for sausage and kink waves are shown in Fig. 2.

Fist of all, all waves propagating in a magnetic tube under coronal conditions are *body* waves, i.e. $\Lambda_0 < 0$ for all these waves. All wave modes can be divided in two classes: *fast* and *slow*. The phase speeds of fast modes are in the interval (V_{A0}, V_{Ae}), while the phase speeds of slow modes are in the interval (C_{T0}, C_{S0}).

It is clear from Fig. 2 that all fast *sausage* modes have a low wavenumber cut-off. Since the cut-off wavenumber for any fast sausage mode is of the order or larger than a^{-1}, it follows that only fast sausage waves with the wavelength of the order of or smaller than the tube radius can propagate in the tube.

Fast *kink* modes starting from the second one have the same properties as the fast sausage modes. However the properties of the first kink mode are completely different. It exists for any value of k. In the long-wavelength approximation its phase speed is equal to the *kink* speed give by

$$C_k = \left(\frac{\rho_0 V_{A0}^2 + \rho_e V_{Ae}^2}{\rho_0 + \rho_e} \right)^{1/2} . \tag{24}$$

To our knowledge this result was first obtained for a tube in a magnetic-free environment by Ryutov and Ryutova (1976). The approximate expression for the phase velocity of the first fast kink wave is (see Edwin and Roberts (1983))

$$\frac{\omega}{k} = C_k \left\{ 1 - \frac{\rho_0 \rho_e (V_{Ae}^2 - V_{A0}^2)}{2 C_k^2 (\rho_0 + \rho_e)^2} \lambda^2 k^2 a^2 K_0(\lambda |k| a) \right\}, \tag{25}$$

where $\lambda = (1 - C_k^2 / V_{Ae}^2)^{1/2}$.

We see that the properties of the first fast kink mode are completely different from those of the other fast body modes. In particular, since the cut-off wavelengths for the fast body modes are of the order of or smaller than the tube radius, and the length of a typical coronal magnetic loop is much larger than its radius, all sausage fast modes and all kink fast modes but the first one can exist in coronal loops only in the form of very high harmonics with respect to z. On the other hand, the oscillations of coronal loops corresponding to the first fast kink mode can contain all harmonics with respect to z, including the fundamental one. To distinguish the first fast kink mode from the other fast kink modes it was suggested by Ruderman and Roberts (2002) to call it the *global* fast kink wave.

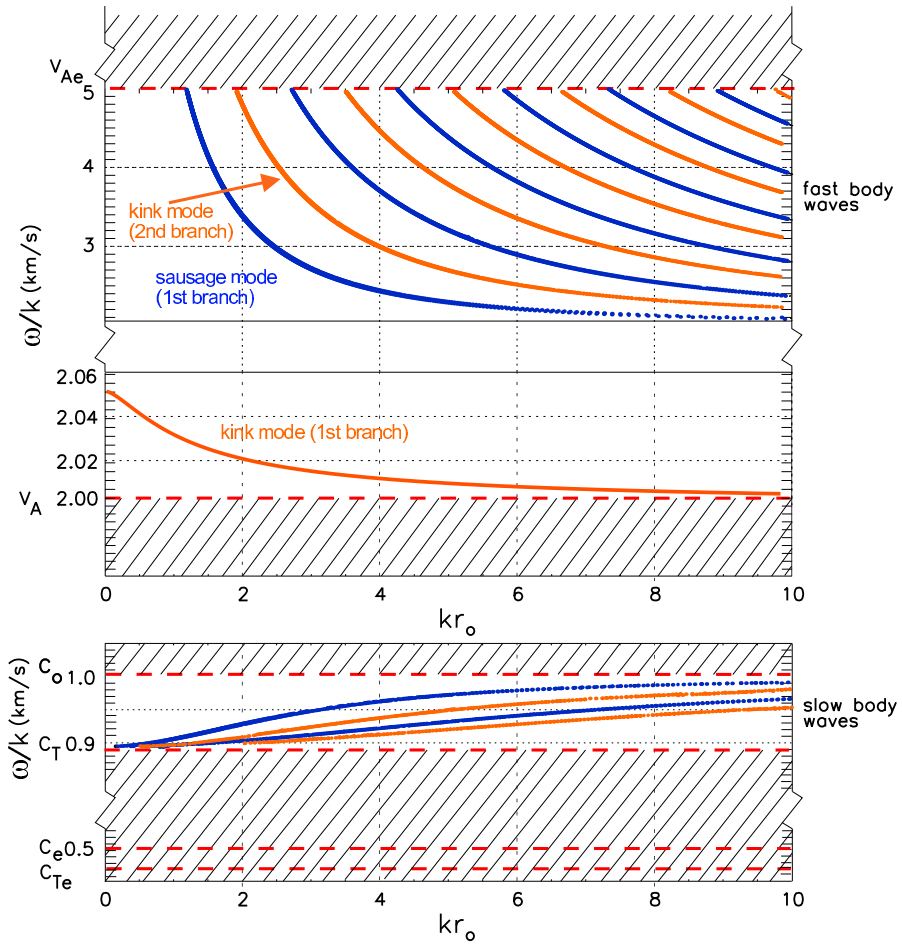

Fig. 2 Typical dependences of mode phase speeds on the wavenumber under coronal conditions ($C_{S0,e} \ll V_{A0}$, $V_{A0} < V_{Ae}$). The slow band is zoomed, and only the first two harmonics of a mode are shown (lower panel).

Let us now discuss the properties of the slow body waves. Typically the plasma in coronal loops is hotter than the surrounding plasma, so that $C_{S0} > C_{Se}$. Since $V_{A0} \gg C_{S0}$ in the corona, the difference between C_{T0} and C_{S0} is very small, so that usually $C_{T0} > C_{Se}$ as well. Then it is straightforward to see that $\Lambda_e^2 > 0$ when $C_{T0} < \omega/k < C_{S0}$ and the slow body waves are evanescent in the external plasma. Since the difference between C_{T0} and C_{S0} is very small, the phase speeds of slow waves only weakly depend on the wavenumber k (see Fig. 2, lower panel). The slow body waves exist for any value of k. The phase speeds of all slow body waves tend to C_{T0} as $ak \to 0$. For more detailed discussion of properties of the slow body waves see, e.g., Zhugzhda and Goossens (2001).

The theory of propagating waves in infinite magnetic tubes homogeneous in the longitudinal direction was extended in many directions. In particular Bennett et al. (1999) and Erdélyi and Fedun (2006, 2007) studied the wave propagation in twisted tubes. Mikhalyaev and Solov'ev (2005) and Carter and Erdélyi (2007) investigated the waves propagating in annular magnetic cylinders with the straight magnetic field lines. Erdélyi and Carter (2006) and Carter and Erdélyi (2008) considered the wave propagation in annular magnetic cylinders with the magnetic field lines twisted in the annulus. We do not discuss these theory extensions here and refer an interested reader to the original papers.

3 Method of asymptotic expansions

In this section we give another derivation of the dispersion relation for the global fast kink waves in the long wavelength approximation. Since this dispersion relation has already been derived in the previous section, it would not make sense to derive it using another method if it would be restricted to the case of a straight homogeneous magnetic tube. However the asymptotic method that we describe in this section allows far going generalisations. In particular, it can be applied to magnetic tubes with the density and radius varying along the tube, and to the tube with magnetic twist. On the other hand, this method is the most transparent when it is applied to a straight homogeneous magnetic tube.

The observed transverse oscillations of coronal loops are standing rather than propagating waves. Of course, in the linear theory of waves in homogeneous magnetic flux tubes there is not very much difference between the two types of waves. A standing wave is just a superposition of two propagating waves. However, when a tube is inhomogeneous in the longitudinal direction, i.e. when the density and/or tube radius varies along the tube, the description of standing waves is different from that of propagating waves. Having the generalisation of the theory for inhomogeneous tubes in mind we consider standing waves in this section. The equilibrium state together with the perturbed tube are shown in Fig. 3. As in the previous section, the tube radius is a, and the plasma density inside and outside the tube is ρ_0 and ρ_e, respectively.

Our aim is to apply theoretical results to the observed transverse oscillations of coronal loops. The phase speed of these oscillations is of the other of Alfvén speed. The plasma pressure in the corona is much smaller than the magnetic pressure. As a result, the Alfvén speed is much larger than the sound speed. This observation enables us to use the cold plasma approximation in what follows. Then it follows from the equilibrium condition (5) that $B_e = B_0 = B$.

The tube length is $2L$. We assume that the magnetic field lines are frozen in the dense photospheric plasma at the tube ends. This implies that the plasma displacement in the direction normal to the equilibrium magnetic field is zero at the tube ends, i.e.

$$\xi_r = 0, \quad \xi_\varphi = 0 \quad \text{at} \;\; z = \pm L. \tag{26}$$

It follows from the last equation in Eq. (11) and Eq. (26) that $b_z = 0$ at $z = \pm L$. Since, in the cold plasma approximation, $P = Bb_z/\mu_0$, we obtain that P satisfies the same boundary condition,

$$P = 0 \quad \text{at} \;\; z = \pm L. \tag{27}$$

In our analysis we use Eqs. (7)-(10). Since $C_S = C_T = 0$ in the cold plasma approximation, it follows from Eq. (10) that $\xi_z = 0$. Now we look for the solutions

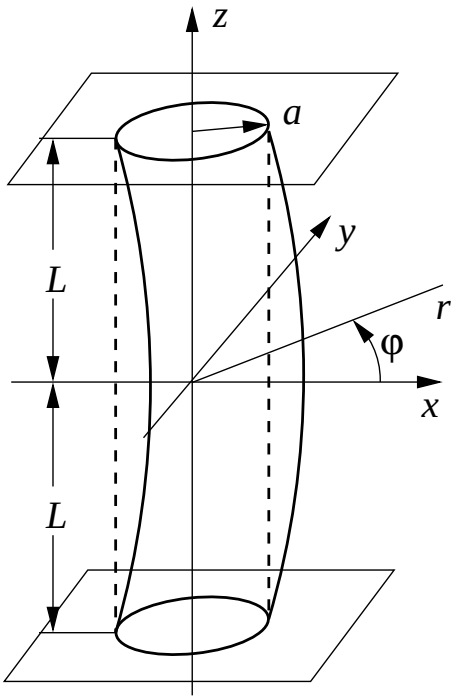

Fig. 3 The equilibrium state and the perturbed tube. The dashed lines show the tube in the equilibrium, while the solid lines show the tube perturbed by the fundamental mode of the global fast kink wave.

describing the eigenmodes of global fast kink oscillations. In accordance with this we take all variables proportional to $\exp[i(-\omega t+\varphi)]$ (i.e. $m=1$). Since the equilibrium quantities are independent of z we also can Fourier-analyse the equations with respect to z. However, having in mind application to tubes inhomogeneous in the longitudinal direction, we do not do this and retain the z-dependence.

Now we recall that the coronal magnetic loops are thin structures with the typical ratio of the transverse size to the length equal to $0.01 \div 0.05$. This fact enables us to use $\epsilon = a/L \ll 1$ as a small parameter in the asymptotic expansions. In order to have the same characteristic lengths for the spatial variables in the longitudinal and transverse direction we introduce the scaled or stretching variable $\zeta = \epsilon z$. The characteristic spatial scale with respect to this variable is $\epsilon L = a$, i.e. it is the same as the characteristic spatial scale with respect to r. The typical value of the oscillation frequency is $\omega = V_A/L = \epsilon^{-1}V_A/a$. This observation implies that we need to introduce the scaled frequency $\Omega = \epsilon^{-1}\omega$. After that Eqs. (7)-(9) reduce to

$$\frac{1}{r}\frac{\partial}{\partial r}\left(r\frac{\partial P}{\partial r}\right) - \frac{P}{r^2} + \epsilon^2\left(\frac{\partial^2 P}{\partial \zeta^2} + \frac{\Omega^2}{V_A^2}\right)P = 0, \tag{28}$$

$$V_A^2\frac{\partial^2 \xi_r}{\partial \zeta^2} + \Omega^2\xi_r = \frac{1}{\epsilon^2\rho}\frac{\partial P}{\partial r}, \tag{29}$$

$$V_A^2 \frac{\partial^2 \xi_\varphi}{\partial \zeta^2} + \Omega^2 \xi_\varphi = \frac{iP}{\epsilon^2 \rho r}. \tag{30}$$

The system of Eqs. (28)-(30) contains the small parameter ϵ^2. This implies that we can look for the solution to this systems in the form of asymptotic expansions with respect to ϵ^2. In what follows we use only the first order approximation, so that we use the same notation P, ξ_r and ξ_φ for the first terms of expansions of P, ξ_r and ξ_φ in the power series with respect to ϵ^2.

In the first order approximation Eq. (28) reduces to

$$\frac{1}{r}\frac{\partial}{\partial r}\left(r\frac{\partial P}{\partial r}\right) - \frac{P}{r^2} = 0. \tag{31}$$

The solution to this equation regular at $r = 0$ and vanishing as $r \to \infty$ is straightforward:

$$P = \begin{cases} A_0(\zeta) r, & r < a, \\ A_e(\zeta) r^{-1}, & r > a, \end{cases} \tag{32}$$

where $A_0(\zeta)$ and $A_e(\zeta)$ are arbitrary functions satisfying the boundary condition (27), $A_0(\pm\epsilon L) = A_e(\pm\epsilon L) = 0$. Substituting Eq. (32) in Eq. (29) we obtain two equations, one valid inside the tube and one outside,

$$V_{A0}^2 \frac{\partial^2 \xi_{r0}}{\partial \zeta^2} + \Omega^2 \xi_{r0} = \frac{A_0}{\epsilon^2 \rho_0}, \tag{33}$$

$$V_{Ae}^2 \frac{\partial^2 \xi_{re}}{\partial \zeta^2} + \Omega^2 \xi_{re} = -\frac{A_e}{\epsilon^2 \rho_e r^2}. \tag{34}$$

It follows from the second boundary condition in (6) that $A_e = a^2 A_0$. Now we substitute this results in Eq. (33) and use and Eqs. (33) and (34) at the boundary, i.e. at $r = a$. Then it follows from the first boundary condition (6) that $\xi_{r0} = \xi_{re}$ and we arrive at

$$V_{A0}^2 \frac{\partial^2 \xi_{r0}}{\partial \zeta^2} + \Omega^2 \xi_{r0} = \frac{A_0}{\epsilon^2 \rho_0}, \quad V_{Ae}^2 \frac{\partial^2 \xi_{r0}}{\partial \zeta^2} + \Omega^2 \xi_{r0} = -\frac{A_0}{\epsilon^2 \rho_e}. \tag{35}$$

Eliminating A_0 from these equations and returning to the original variables we obtain

$$\frac{d^2 \xi_{r0}}{dz^2} + \frac{\omega^2}{C_k^2} \xi_{r0} = 0, \tag{36}$$

where the kink speed C_k is given by Eq. (24). The solution to Eq. (36) has to satisfy the first boundary condition in (26). Equation (36) together with this boundary condition constitute the Sturm-Liouville problem for the function $\xi_{r0}(z)$. In accordance with our derivation Eq. (36) is only valid at $r = a$. However, it follows from Eq. (33) that ξ_{r0} is independent of r, so that Eq. (36) is valid for any $r \le a$. It follows from Eqs. (30) and (32) that $\xi_{\varphi 0}$ is also independent of r. Hence, the plasma displacement inside the tube is independent of r.

The solution to Eq. (36) is given by

$$\xi_{r0} = q_1 \cos(\omega z / C_k) + q_2 \sin(\omega z / C_k),$$

where q_1 and q_2 are arbitrary constants. Substituting this solution in the first boundary condition in (26) we obtain

$$\omega = C_k k_n, \quad k_n = \frac{\pi(n+1)}{2L}, \quad (n = 0, 1, \dots). \tag{37}$$

Here $n = 0$ corresponds to the fundamental mode and $n > 0$ to the nth overtone. In addition we obtain that $q_2 = 0$ when n is even, so that

$$\xi_{r0} = q_1 \cos(k_n z). \tag{38}$$

When n is odd we have $q_1 = 0$ and

$$\xi_{r0} = q_2 \sin(k_n z). \tag{39}$$

Let us now investigate the polarisation of the eigenmodes. Up to now in this section ξ_{r0} and $\xi_{\varphi 0}$ were Fourier coefficients in the expansions of the radial and azimuthal components of the plasma displacement in the Fourier series with respect to t and φ. Now we use this notation for the components of the plasmas displacement in the physical space. We drop the subscript '0' because we will consider only the plasma displacement inside the tube. Keeping in mind that both ξ_r and ξ_φ are proportional either to $\cos(k_n z)$ or to $\sin(k_n z)$, we will drop this multiplier in the expressions for these quantities. Then, for the kink oscillation, we can write $\xi_r = q(t)e^{i\varphi} + q^*(t)e^{-i\varphi}$, where the asterisk indicates the complex conjugate. It follows from Eqs. (29) and (30) that $\xi_\varphi = iq(t)e^{i\varphi} - iq^*(t)e^{-i\varphi}$. Since we consider an eigenmode, it follows that $q(t) = q_+ e^{i\omega t} + q_- e^{-i\omega t}$, where ω is given by Eq. (37). Substituting this expression in the expressions for ξ_r and ξ_φ we eventually arrive at

$$\begin{aligned} \xi_r &= A_+ \cos(\omega t + \varphi + \alpha_+) + A_- \cos(\omega t - \varphi + \alpha_-), \\ \xi_\varphi &= -A_+ \sin(\omega t + \varphi + \alpha_+) + A_- \sin(\omega t - \varphi + \alpha_-), \end{aligned} \tag{40}$$

where $A_\pm$ and $\alpha_\pm$ are arbitrary constants. Let us introduce the auxiliary Cartesian coordinates x, y, z. Then

$$\begin{aligned} \xi_x = \xi_r \cos\varphi - \xi_\varphi \sin\varphi &= A_+ \cos(\omega t + \alpha_+) + A_- \cos(\omega t + \alpha_-) \\ &= Q_x \cos(\omega t + \alpha_x), \end{aligned} \tag{41}$$

$$\begin{aligned} \xi_y = \xi_r \sin\varphi + \xi_\varphi \cos\varphi &= -A_+ \sin(\omega t + \alpha_+) + A_- \sin(\omega t + \alpha_-) \\ &= Q_y \cos(\omega t + \alpha_y). \end{aligned} \tag{42}$$

The quantities Q_x, Q_y, α_x and α_y are expressed in terms of $A_\pm$ and $\alpha_\pm$. We do not give these expressions because they are not used in what follows. Since $A_\pm$ and $\alpha_\pm$ are arbitrary constants, Q_x, Q_y, α_x and α_y are also arbitrary constants.

Equations (41) and (42) show that the plasma displacement $\boldsymbol{\xi}$ is independent of r and φ inside the tube, i.e. the tube is oscillating like a solid string. Hence, it is enough to consider the motion of the tube axis only. In general, Eqs. (41) and (42) describe elliptically polarised motion, so that each point of the tube axis is moving along an ellipse in the plane perpendicular to the tube axis. If we take two arbitrary points, $z = z_1$ and $z = z_2$ on the tube axis, then the corresponding ellipses are similar, i.e. they have the same ratio of the axes, and the axis directions are also the same, and only the magnitude of the large axis varies with z. What is also important, at a fixed moment of time, the displacements of these two points are either parallel or antiparallel to each other. In particular, they are strictly parallel in the fundamental mode.

4 Effects of stratification and expansion

The typical height of the apex point of a coronal loop is 100 Mm, which is about twice larger than the atmospheric scale height in the corona. This means that the plasma density can vary along the loop by an order of magnitude. Hence, it is important to study the effect of the density variation on the transverse coronal loop oscillations. This problem was first addressed by Andries et al. (2005b). These authors expanded the dependent variables in the generalised Fourier series with respect to the eigenmodes of the Alfvén operator. Substituting these expansions in the linearised MHD equations they reduced the problem to evaluation of the eigenvalues of an infinite matrix. The eigenfrequencies of the stratified coronal loop are equal to the square roots from the eigenvalues. To solve this problem the authors truncated the infinite matrix and reduced it to a finite square matrix. The equation determining the eigenfrequencies is obtained by equating the determinant of this matrix to zero. Since the elements of the determinant depend nonlinearly on the eigenfrequency, this approach resulted in a complicated algebraic equation that had to be solved numerically. The most important result obtained by Andries et al. (2005b) was that the overtone frequencies of a stratified magnetic loop are, in general, not multiple of the fundamental frequency. In particular, the first overtone frequency is smaller than the double fundamental frequency.

The method used by Andries et al. (2005b) is applicable to stratified magnetic loops with arbitrary ratio of the radius and length. However, as we have already pointed out, for typical coronal loops, this ratio is very small and can be used as a small parameter. Dymova and Ruderman (2005) used this fact to develop the asymptotic theory of oscillations of stratified magnetic loops. Their analysis is almost complete repetition of the analysis presented in the previous section for homogeneous magnetic tubes. As a result, they obtain the same equation (36), however with C_k depending on z. The quantity C_k is still given by equation (24). It depends on z because ρ_0 and ρ_e are functions of z. The numerical solution of the eigenvalue problem for equation (36) with $C_k = C_k(z)$ is trivial. In some cases this eigenvalue problem can even be solved analytically. One such example is given by Dymova and Ruderman (2006a) where the equation derived by Dymova and Ruderman (2005) was applied to studying the kink oscillations of stratified coronal loops. In this example the density inside the loop is given by

$$\rho_i(z) = \frac{\rho_a}{[1-(1-\kappa)(z/L)^2]^2}, \tag{43}$$

where L is the half-length of the loop, ρ_a the density at the apex point, ρ_f the density at the foot points, and $\kappa = \sqrt{\rho_a/\rho_f}$. The density outside the loop is given by $\rho_e(z) = \chi\rho_i(z)$, where $\chi < 1$ is a constant. In that case the solution of equation (36) with $C_k(z)$ given by (24) can be found analytically, and the eigenfrequencies of the loop oscillations are given by

$$(\omega_{0n}^e)^2 = \frac{\pi B^2 a^2\sqrt{1-\kappa}}{\mu_0 ML(1+\chi)}\left(\frac{2\sqrt{1-\kappa}}{\kappa} + \ln\frac{1+\sqrt{1-\kappa}}{1-\sqrt{1-\kappa}}\right) \times \left\{\pi^2(2n-1)^2\left(\ln\frac{1+\sqrt{1-\kappa}}{1-\sqrt{1-\kappa}}\right)^{-2} + 1\right\}, \quad n = 1, 2, \ldots, \tag{44}$$

for even modes (i.e., the fundamental mode, the second overtone, etc.), and by

$$(\omega_{0n}^{o})^2 = \frac{\pi B^2 a^2 \sqrt{1-\kappa}}{\mu_0 M L (1+\chi)} \left(\frac{2\sqrt{1-\kappa}}{\kappa} + \ln \frac{1+\sqrt{1-\kappa}}{1-\sqrt{1-\kappa}} \right) \times \left\{ 4\pi^2 n^2 \left(\ln \frac{1+\sqrt{1-\kappa}}{1-\sqrt{1-\kappa}} \right)^{-2} + 1 \right\}, \quad n = 1, 2, \ldots, \tag{45}$$

for odd modes (i.e., the first, third, and so on overtones). In equations (44) and (45) B is the equilibrium magnetic field and M is the total mass of plasma inside the loop given by

$$M = \pi a^2 L \rho_a \left(\frac{1}{\kappa} + \frac{1}{2\sqrt{1-\kappa}} \ln \frac{1+\sqrt{1-\kappa}}{1-\sqrt{1-\kappa}} \right). \tag{46}$$

When $\kappa \to 1$, which corresponds to the limit of a non-stratified loop, we obtain from equations (44) and (45) the familiar expressions for the eigenfrequencies, $\omega_{0n}^{e} = \pi C_k (2n-1)/2L$ and $\omega_{0n}^{o} = \pi C_k n/L$.

Dymova and Ruderman (2006a) also carried out the calculations of eigenfrequencies for the same dependence of the density on z as that used by Andries et al. (2005b) and compared their results with those obtained by Andries et al. (2005b). The difference in the eigenmode frequencies calculated by the two methods was less than 1% for $a/L \lesssim 0.05$, so that the accuracy of the asymptotic theory is very good.

Another example of analytical solution of the eigenvalue problem for equation (36) is given by Verth at al. (2007) who considered a piecewise-constant density profile.

Observations show that the loop radius does not vary very much along the loop. Still the ratio of the loop radius at the apex point to that at the foot points can be up to 2 (e.g. **?**Verth and Erdélyi (2008)). This corresponds to the increase in the loop cross-section area up to four times and, in accordance with the magnetic flux conservation, to the same decrease in the magnetic field magnitude. The increase in the loop mass due to its expansion and the decrease in the magnetic field magnitude can substantially affect the eigenfrequencies of the loop oscillations, so that this effect deserves attention. Transverse oscillations of stratified coronal loops with the variable cross-section were studied by Verth and Erdélyi (2008) and Ruderman et al. (2008). Once again only long loops were considered and the asymptotic theory of transverse oscillations of such loops was developed. While it was assumed by Verth and Erdélyi (2008) that the expansion factor (the ratio of the loop radii at the apex and foot points) is small, Ruderman et al. (2008) studied oscillations of loops with arbitrary expansion factor. The analysis by Ruderman et al. (2008) is much more involved than that in the previous section of this paper. The reason is as follows. The boundary of an expanding loop is determined by $r = f(z)$ in cylindrical coordinates. It is inconvenient to solve MHD equations in a region with the boundary of this form. To avoid this problem it was noticed that the equilibrium magnetic flux function ψ is constant at the loop boundary. This function was used as a new independent variable instead of r. In the new variables the loop boundary is determined by $\psi = \psi_0 = \text{const}$. However, the MHD equations in coordinates ψ, φ, z are more complicated than in coordinates r, φ, z.

The main result obtained by Ruderman et al. (2008) is the following. The squares of eigenfrequencies of transverse oscillations of stratified magnetic loops with the variable cross-sections are the eigenvalues of the Sturm-Liouville problem

$$\frac{d\eta}{dz^2} + \frac{\omega^2}{C_k^2}\eta = 0, \quad \eta = 0 \ \text{ at } \ z = \pm L, \tag{47}$$

where $\eta = \xi_{r0}/a$ and $a = a(z)$ is the (variable) loop radius. Formally equation (47) is the same as the equation for stratified loops with constant cross-section. The fact that it is written for $\eta = \xi_{r0}/a(z)$ affects only the shape of eigenfunctions, but does not affect the eigenfrequencies. However the properties of eigenfrequencies of loops with the variable cross-section still can differ very much from those of loops with the constant cross-section. The reason is that, for loops with the variable cross-section, in the expression (24) for C_k not only the densities ρ_i and ρ_e but also the equilibrium magnetic field B is a function of z. In accordance with the magnetic flux conservation $B = \mathrm{const}/a^2(z)$. In loops with the constant cross-section C_k increases monotonically with the height in the atmosphere. The most important consequence of this behaviour is that the ratio of frequencies of the first overtone and the fundamental mode is less than 2. The behaviour of C_k in loops with the variable cross-section can be much more complex. As a result the ratio of frequencies of the first overtone and the fundamental mode can be larger or equal to 2. For example, it is exactly equal to 2 when $a^4(\rho_i + \rho_e) = \mathrm{const}$ because in this case $C_k = \mathrm{const}$. The implication of this result on coronal seismology will be discussed in Sect. 11.

A more detailed discussion of transverse oscillations of coronal loop with the density varying along the loop is guven by Andries et al. (2009).

5 Kink oscillations of twisted tubes

If we assume that the equilibrium magnetic field in a magnetic configuration with a straight magnetic tube (even with the variable cross-section) is potential (i.e. there is no electrical current), then we immediately obtain that it is untwisted, i.e. the azimuthal component of the equilibrium magnetic field is zero. However at present there is no observational evidence that the coronal loops are current-free. Moreover, it seems that the observed very low expansion factors of coronal loops (close to unity) give the evidence in favour of presence of some currents in the coronal loops.

Further, granular shear motion, differential rotation or meridional circulation in the photosphere can introduce a twist to the flux tubes from pores to sunspots. Erupting prominences or CMEs, with their footpoints anchored in the dense sub-photosphere, often appear to have twisted field lines. It is natural and practical to extend the investigations of MHD wave modes to twisted magnetic flux tubes. These arguments make studying oscillations of twisted coronal loops topical.

Twisted tubes have been studied before but mainly in terms of stability. In accordance with the Shafranov-Kruskal stability criterion a twisted magnetic tube can be stable only if the twist is not very strong. In particular, for a long tube, it follows from this criterion that the tube can be stable only if the ratio of the azimuthal component of the equilibrium magnetic field, B_φ, to the magnetic field magnitude is of the order of or smaller than a/L, $B_\varphi/B \lesssim a/L$.

As we have already mentioned in Sect. 1, propagating kink waves in straight twisted unstratified magnetic tubes were studied by Bennett et al. (1999), Erdélyi and Carter (2006), Erdélyi and Fedun (2006, 2007) and Carter and Erdélyi (2008). A sketch of the equilibrium state with a twisted magnetic tube is shown in Fig. 4. In the cold plasma approximation the magnetic field has to satisfy the equilibrium condition inside the tube,

$$\frac{dB_i^2}{dr} + \frac{2B_{i\varphi}^2}{r} = 0, \tag{48}$$

where $B_i^2 = B_{i\varphi}^2 + B_{iz}^2$, and the conditions of magnetic pressure balance at the tube boundary given by Eq. (5) with $p_0 = p_e = 0$.

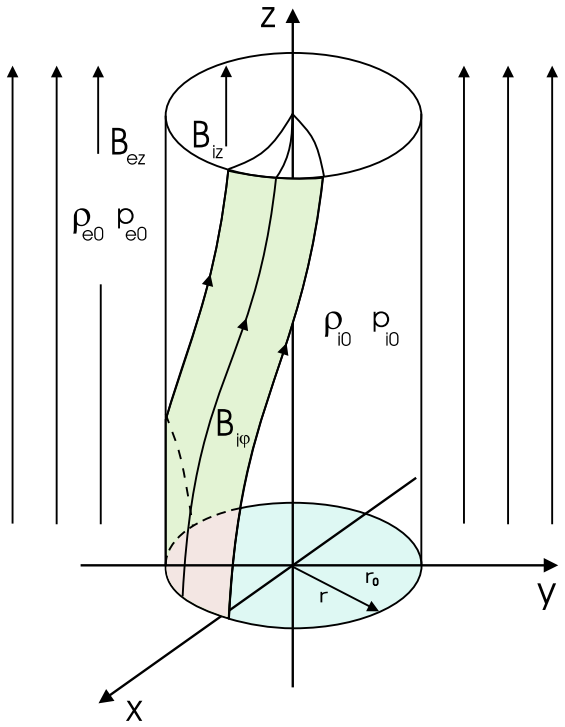

Fig. 4 The equilibrium configuration with a twisted magnetic tube. When the tube is thin and the Shafranov-Kruskal stability criterion is satisfied, $B_{iz} = B_{ez} + \mathcal{O}(a^2/L^2)$ in the cold plasma approximation.

There is no difference in studying propagating and standing waves in untwisted magnetic tubes. A standing wave is obtained by the superposition of two waves with the same frequencies and wavenumbers propagating in the opposite directions. The presence of twist brakes the symmetry of wave propagation with respect to the change of the propagation direction. Hence, in general, a standing wave in a twisted tube cannot be obtained in the same simple way as in an untwisted tube. It can be shown that a standing wave is now a superposition of two propagating waves with the same frequencies but with different wave numbers. Hence, in principle, studying standing waves in a straight twisted unstratified magnetic tube still can be reduced to studying propagating waves. However, it is more convenient to study the standing waves directly.

The situation becomes even more complicated when a magnetic tube is stratified. In this case only the direct study of standing waves is convenient. The standing kink oscillations of straight twisted stratified magnetic tubes with the constant cross-section were studied by Ruderman (2007). Once again the investigation was restricted to thin tubes, $a \ll L$. When the tube is thin it follows from Eqs. (5) and (48) that $B_{iz} = B_e + \mathcal{O}(a^2/L^2)$. The asymptotic analysis similar to one described in Sect. 3 was carried

out. This analysis has shown that, under the assumption $B_\varphi/B \lesssim a/L$, the kink oscillations are described by the same Sturm-Liouville problem as those in a non-twisted tube. Hence, a week twist can only result in corrections to the eigenvalues and eigenfrequencies that are smaller than or of the order of $(a/L)^2$. Such corrections are negligible in applications to the coronal magnetic loops.

6 The effect of curvature

In all models that we discussed up to now magnetic tubes were assumed to be straight. However, real coronal magnetic loops are curved. What is the effect of this curvature on the kink oscillations? This problem was first addressed by Van Doorsselaere et al. (2004b). These authors considered a model of a coronal loop that has the shape of a half-torus. They neglected the density stratification. Using the toroidal coordinates they solved this problem analytically in the thin tube approximation. The main results obtained in this study can be summarised as follows. The kink modes of a straight tube with a circular cross-section are degenerate in a sense that they can be polarised in any direction. In contrast, the kink eigenmodes of a curved tube can be polarised either in the plane of the tube (vertical oscillations), on in the direction perpendicular to the plane of the tube (horizontal oscillations). The frequencies of the two kink modes polarised in the mutually orthogonal directions are different. However the difference between these two frequencies is of the order of $(a/L)^2$, i.e. it is very small for coronal magnetic loops. Recently we were informed by the authors that they found an error in their analysis, and now they are preparing a corrected version of their paper. However, to our knowledge, this error does not affect the main conclusion made by Van Doorsselaere et al. (2004b).

Terradas et al. (2006) studied the same problem numerically taking the density stratification into account. They obtain the results similar to those obtained by Van Doorsselaere et al. (2004b). More detailed discussion of the curvature effect can be found in the review paper by Van Doorsselaere et al. (2009) in this issue.

It is worth noting that the majority of the observed transverse oscillations of coronal magnetic loops are horizontally polarised. However Wang and Solanki (2004) reported the observations by TRACE of the vertically polarised oscillations of coronal loops (see also Wang et al. (2008)).

7 Kink oscillations of coronal loops with non-circular cross-section

It was assumed in the majority of theoretical studies that coronal loops have circular cross-sections. However, at present there are no observational evidences that this is correct. Measuring the parameters of the loop cross-section demands observations with a very high resolution not available at present. For correct interpretation of observational data we need robust models that do not change very much when assumptions used to develop these models are relaxed. From this point of view it is very important to investigate how much the theoretical results concerning the kink coronal loop oscillations depend on the assumption that the loop cross-section is circular. The first insight in this problem was made by Ruderman (2003) who studied the kink oscillations of a homogeneous magnetic tube with the elliptic cross-section. It was shown that, in the cold plasma approximation, there are two fast kink modes polarised along

the small and large axis of the elliptic cross-section. In the thin tube approximation the frequencies of these modes are given by

$$\omega_{k1}^2 = \frac{\rho V_A^2 k^2 (a+b)}{b\rho_i + a\rho_e}, \quad \omega_{k2}^2 = \frac{\rho V_A^2 k^2 (a+b)}{a\rho_i + b\rho_e}. \tag{49}$$

Here a and b are the large and small half-axes of the elliptic cross-section, $k = \pi/L$ and L is the loop length. The frequencies ω_{k1} and ω_{k2} correspond to oscillations polarised along the small and large axes. Note that $\omega_{k2} < \omega_{k1}$. When $a = b$, $\omega_{k1} = \omega_{k2} = \omega_k$. The two fundamental kink modes of a tube with the elliptic cross-section are shown in Fig. 5.

Recently the eigenmodes of a homogeneous magnetic tube with the elliptic cross-section were studied in a plasma with the finite pressure by Erdélyi and Morton (2009). Since the account of finite pressure is mainly important for sausage modes and practically does not affect the fast kink modes we do not discuss in detail the results of this study here, and only reproduce their figure showing the dispersion curves of different modes for the values of parameters relevant for the solar corona. In Figure 6 the dispersion curves marked as "$\mathrm{kink_m}$ (1st branch)" and "$\mathrm{kink_M}$ (1st branch)" correspond to the fast global kink modes polarised along the small and large axes of the elliptic cross-section respectively. In the limit $ak \to 0$ their frequencies are equal to ω_{k1} and ω_{k2}. Note that the slow modes do not exist in the cold plasma approximation.

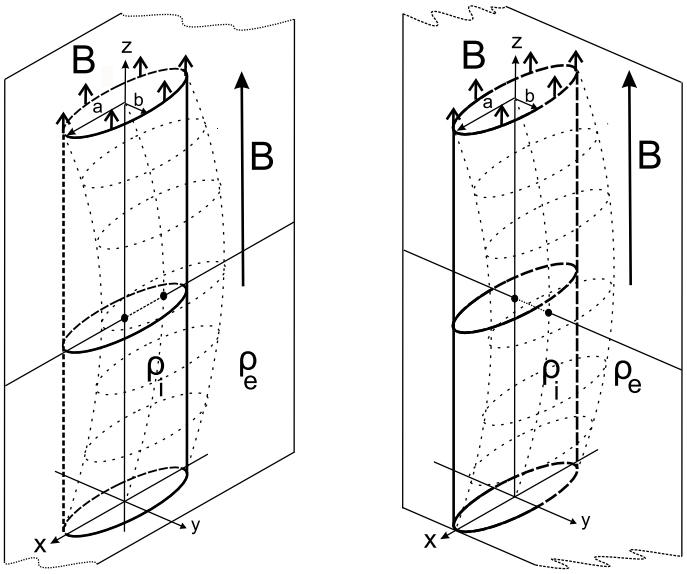

Fig. 5 Sketch showing the equilibrium (bold solid and dashed lines) and perturbed states (thin dashed lines) of a magnetic flux tube with plasma density ρ_i embedded in plasma with density ρ_e. The left hand sketch shows the kink perturbation polarised along the large axis of the elliptic cross-section, and the right one shows the kink perturbation polarised along the small axis. The plane in which the kink modes are polarised is shown.

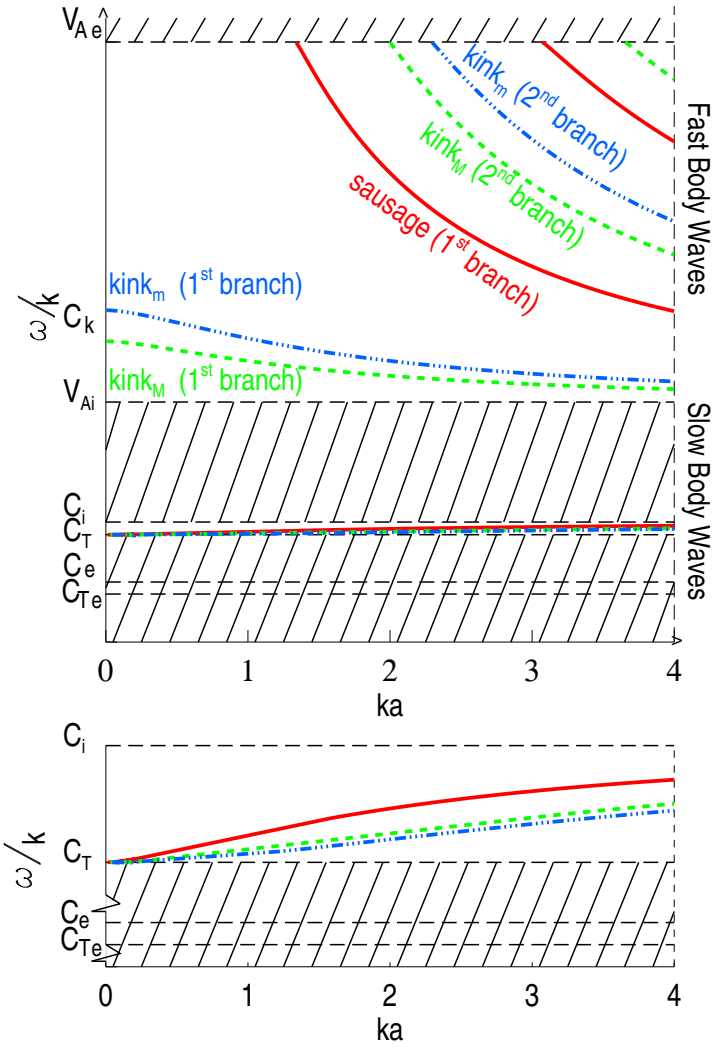

Fig. 6 The dispersion curves for waves propagating in a tube with the elliptic cross-section. The dispersion curves marked as "$\mathrm{kink_m}$ (1st branch)" and "$\mathrm{kink_M}$ (1st branch)" correspond to the fast global kink modes polarised along the small and large axes of the elliptic cross-section respectively. The lower part of the figure shows the magnified dispersion curves for flow modes. Note that these modes do not exist in the cold plasma approximation.

8 Kink oscillations in annular magnetic cylinders

Sub-resolution flux tube structure is still a matter of speculations. It is anticipated that the recently launched Hinode/SOT may advance the research on the internal structure of solar magnetic flux tubes. As a specific example, let as recall an interesting earlier observation by Robbrecht et al. (2001): combined data of May 13 1998 from both the

EIT instrument on SOHO and from TRACE show the simultaneous observation of two slow magnetosonic waves propagating along a perceived coronal loop with speeds of 95 and 110 km/s. This observation was interpreted by the authors as temperature differences within the observed loop hinting at a substructure of perhaps either concentric shells of different temperatures or of thin strands within the same loop at different temperatures. There is no conclusive proof disputing these possible flux tube structures nor preference given towards one in particular.

In this section we consider the wave propagation in a core magnetic cylinder surrounded by a concentric shell. Such a magnetic plasma configuration can be called an annular magnetic cylinder. The geometry of the model is shown in Fig. 7. The magnetic field is in the direction of the cylinder axis and its magnitude is B_i in the core cylinder, B_0 in the annulus, and B_e in the external plasma. The plasma densities in these three regions are ρ_i, ρ_0 and ρ_e respectively, and we assume that $\rho_i, \rho_0 > \rho_e$.

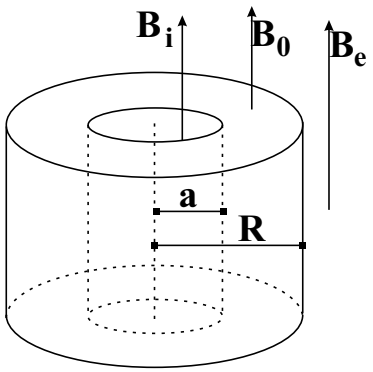

Fig. 7 The equilibrium configuration of a magnetic cylinder consisting of a core, annulus and external regions, all with straight magnetic field.

At present only the propagating waves in annular magnetic cylinders were studied. But, since in magnetic plasma configurations with straight magnetic field lines a standing wave is a superposition of two propagating waves with the same frequencies and opposite wavenumbers, it is straightforward to apply the results of this study to kink oscillations of annular magnetic cylinders. The propagating waves in annular magnetic cylinders were studied by Carter and Erdélyi (2007) in the approximation of incompressible plasma, while Mikhalyaev and Solov'ev (2005) took the plasma compressibility into account. Since the cold plasma approximation is quite suitable for the description of the fast kink oscillations of coronal loops, in what follows we use the results obtained by Mikhalyaev and Solov'ev (2005).

One of the consequences of the cold plasma approximation is that the magnetic field magnitude is the same in the core cylinder, the annulus and the external plasma, so that $B_i = B_0 = B_e = B$. Mikhalyaev and Solov'ev (2005) derived the dispersion equation for the fast kink modes in the thin tube approximation. In the cold plasma

approximation this dispersion equation reduces to

$$\left[R^2(\rho_0+\rho_i)(\rho_0+\rho_e)-a^2(\rho_0-\rho_i)(\rho_0-\rho_e)\right]\omega^4 - \frac{2}{\mu_0}R^2B^2k^2(2\rho_0+\rho_i+\rho_e)\omega^2+\frac{4}{\mu_0^2}R^2B^4k^4=0, \tag{50}$$

where k is the wavenumber in the longitudinal direction. For the fundamental mode $k=\pi/L$, where L is the length of the annulus cylinder. The solutions to the dispersion equation (50) are

$$\omega_\pm^2 = V_{Ai}^2k^2R\left[(1+2\chi_0+\chi_e)R\pm\sqrt{(1-\chi_e)^2(R^2-a^2)+(1-2\chi_0+\chi_e)^2a^2}\right] \times\left[(1+\chi_0)(\chi_0+\chi_e)R^2+(1-\chi_0)(\chi_0-\chi_e)a^2\right]^{-1}, \tag{51}$$

where

$$V_{Ai}^2=\frac{B^2}{\mu_0\rho_i},\quad \chi_0=\frac{\rho_0}{\rho_i},\quad \chi_e=\frac{\rho_e}{\rho_i}.$$

When $2\chi_0<1+\chi_e$, in the wave mode with the oscillation frequency ω_- the core cylinder and the annulus oscillate in phase. We will call this mode the *phase* mode in what follows. The displacement of the core cylinder and the annulus in this wave mode are schematically shown on the left panel of Fig. 8. When $a=R$, i.e. there is no annulus, $\omega_-=\omega_k$ and this wave mode becomes the global fast kink mode of a homogeneous tube. In the wave mode with the oscillation frequency ω_+ the core cylinder and the annulus oscillate in antiphase. We will call this mode the *antiphase* mode in what follows. The displacement of the core cylinder and the annulus in this wave mode are schematically shown on the right panel of Fig. 8. When $a=R$, i.e. there is no annulus, this wave mode does not exist.

When $2\chi_0>1+\chi_e$, the situation is reversed. Now the antiphase mode has the frequency ω_-, while the phase mode has the frequency ω_+.

It is straightforward to show that $\omega_\pm^2<V_{Ae}^2=V_{Ai}^2/\chi_e$, so that both the phase and antiphase modes are evanescent in the external plasma. When $\chi_0\neq1$, i.e. there is the annulus, the frequencies ω_- and ω_+ satisfy the inequalities

$$k\min(V_{Ai},V_{A0})<\omega_-<k\max(V_{Ai},V_{A0}), \tag{52}$$

$$\omega_+>k\max(V_{Ai},V_{A0}). \tag{53}$$

where $V_{A0}^2=V_{Ai}^2/\chi_0$. The inequality (53) implies that the wave mode with the frequency ω_+ is a body wave both in the core cylinder and in the annulus. On the other hand, it follows from the inequality (51) that the wave mode with the frequency ω_- is a body wave in the core cylinder and a surface wave in the annulus when $V_{Ai}<V_{A0}$, while it is a surface wave in the core cylinder and a body wave in the annulus when $V_{Ai}>V_{A0}$. Such a wave mode is called *mixed*.

Let us consider one example relevant for the corona. If we take $R=2a$, $\chi_0=0.5$ and $\chi_e=0.1$, then $\omega_+/\omega_-\approx0.677$. We see that the two frequencies can be substantially different.

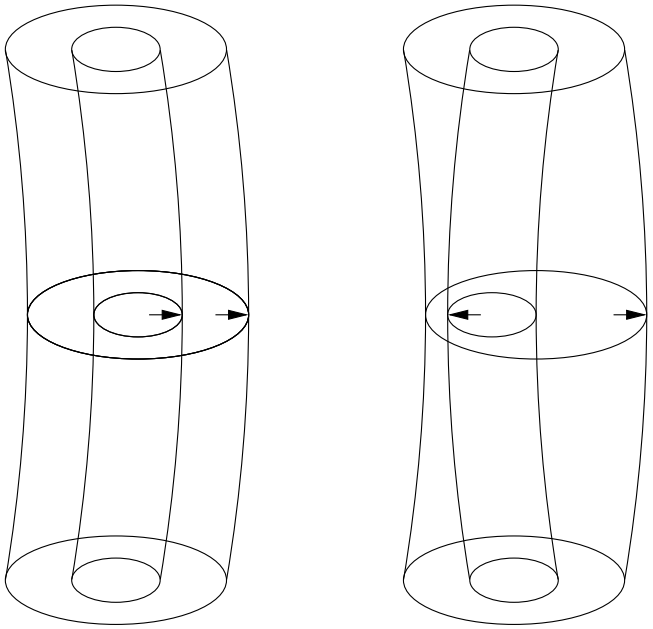

Fig. 8 The kink modes of the annular cylinder oscillation. The left panel corresponds to the mode where the core cylinder and the annulus oscillate in phase. In the thin tube approximation the frequency of this mode is equal to ω_- when $2\rho_0 < \rho_i + \rho_e$ and ω_+ when $2\rho_0 > \rho_i + \rho_e$. The right panel corresponds to the mode where the core cylinder and the annulus oscillate in antiphase. In the thin tube approximation the frequency of this mode is equal to ω_+ when $2\rho_0 < \rho_i + \rho_e$ and ω_- when $2\rho_0 > \rho_i + \rho_e$. The arrows show the plasma displacement.

9 Collective kink oscillations of two parallel coronal loops

Very often it is observed that not a single loop, but a whole array of loops oscillates after being perturbed by, e.g., a solar flare. Moreover, it has been suggested by, e.g., Aschwanden et al. (2000) that the loops as we see them actually consist of a multitude of individual loop strands. These considerations put on the agenda studying collective oscillations of an array of coronal loops. A natural first step in this study is the investigation of collective oscillations of a system of two coronal loops. Recently such an investigation has been carried out numerically by Luna et al. (2008). These authors considered oscillations of two identical homogeneous parallel magnetic tubes with fixed ends. They studied both the eigenmodes of oscillations of this system, and solved the initial value problem. Their main results concerning the eigenmodes can be summarised as follows. There are four fundamental eigenmodes of the system oscillation with respect to the longitudinal direction. In two of these four modes the tubes oscillate in the direction connecting the tube axes, which is denoted as the x-direction, and in two other modes in the perpendicular direction, which is denoted as the y-direction. In each of the two pairs of modes the tubes can oscillate either in the same direction, and in this case they are called symmetric, or in the opposite directions, in which case they are called antisymmetric. Luna et al. (2008) used the notation S_x, A_x, S_y and A_y for this modes, where S and A stay for symmetric and antisymmetric respectively, and

the subscripts 'x' and 'y' indicate the mode polarisation (i.e. the direction of the tube displacement). If we denote the oscillation frequencies of the these four fundamental modes as ω_{Sx}, ω_{Ax}, ω_{Sy} and ω_{Ay} respectively, then they satisfy the following ordering,

$$\omega_{Sx} < \omega_{Ay} < \omega_{Sy} < \omega_{Ax}. \tag{54}$$

When the separation between the tubes increases, all four frequencies tend to the common kink frequency of the two tubes.

Van Doorsselaere et al. (2008) studied this problem analytically in the thin tube approximation. In this paper the oscillations of two parallel loops with arbitrary radii and densities inside them have been considered. The equilibrium configuration is shown in Fig. 9. The coronal loops are modelled by straight homogeneous magnetic tubes. The length of the tube is L. The tube radii are R_L and R_R, and the plasma densities inside the tubes are ρ_L and ρ_R. The density of the plasma outside the tubes is ρ_e, and it is assumed that $\rho_{L,R} > \rho_e$. The distance between the tube axes is $d > R_L + R_R$. The magnetic field is parallel to the tube axes. Since the cold plasma approximation is used, its magnitude, B, is the same everywhere.

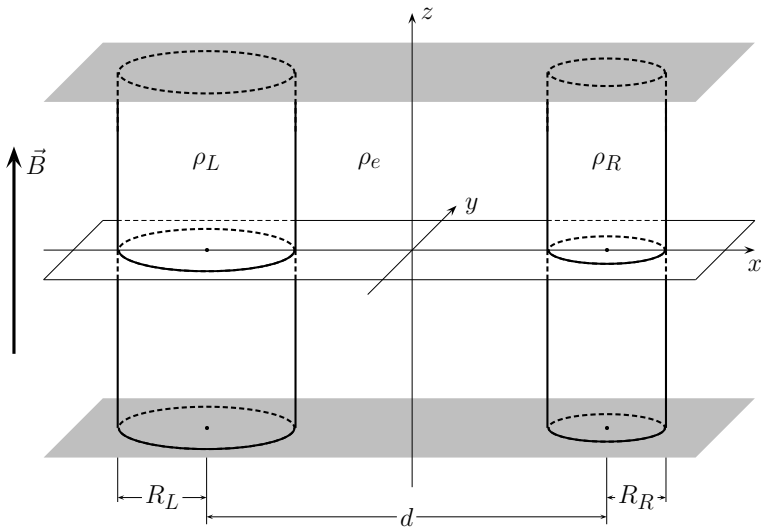

Fig. 9 The equilibrium with two parallel homogeneous magnetic tubes.

It was assumed that the transversal size of the system is much smaller than the tube length. This condition can be written as $d/L = \epsilon \ll 1$. Then the solution was found in the first order approximation with respect to ϵ. For the analytical solution of the problem the bi-cylindrical coordinate system was used. When the tubes are identical, the obtained analytical results are quite similar to the numerical results obtained by Luna et al. (2008). Once again the four modes, S_x, A_x, S_y and A_y, were identified. However, there is one difference between the analytical and numerical results. It was obtained in the analytical investigation that

$$\omega_- = \omega_{Sx} = \omega_{Ay} < \omega_{Sy} = \omega_{Ax} = \omega+, \tag{55}$$

where

$$\omega_{\pm}^2 = \frac{\rho_e V_{Ae}^2 k^2}{(\rho_L+\rho_e)(\rho_R+\rho_e)-(\rho_L-\rho_e)(\rho_R-\rho_e)E^2} \times \left\{\rho_L+\rho_R+2\rho_e \pm \sqrt{(\rho_L-\rho_R)^2+4(\rho_L-\rho_e)(\rho_R-\rho_e)E^2}\right\}. \quad (56)$$

In this expression the quantity $0 < E < 1$ is defined by the geometrical parameters of the equilibrium state. We do not give the expression for E because otherwise we would have to present too many details of the mathematical analysis of the problem. This expression can be found in Van Doorsselaere et al. (2008).

Hence, not four but only two eigenfrequencies have been found in the analytical study. We attribute this difference between the analytical and numerical results to the fact that the eigenfrequencies were calculated analytically only in the first order approximation with respect to ϵ. Our conjecture is that the frequencies ω_{Sx} and ω_{Ay} will split in the next order approximation, and so will ω_{Sy} and ω_{Ax}.

When the tubes are not identical the properties of the two tube system are more complicated. In this case, depending on the geometrical and physical parameters of the system, it can have either standard or anomalous behaviour. The systems with the standard behaviour have the same eigenmodes as the system of two identical tubes. However the systems with anomalous behaviour have two eigenmodes of the Ax-type, and two of Sy-type, while they do not have the Sx and Ay-type modes at all. We denote the four eigenmodes in this case as Axs, Axf, Sys and Syf. Their frequencies satisfy

$$\omega_- = \omega_{Axs} = \omega_{Sys} < \omega_{Syf} = \omega_{Axf} = \omega_+. \quad (57)$$

The distinctive property of the anomalous systems is that the Alfvén frequency in one of the two tubes is larger than ω_-. In the standard systems the Alfvén frequencies in both tubes are smaller than ω_-.

10 Damping of kink oscillations of coronal loops

The observed kink oscillations are strongly damped. First this was reported by Aschwanden et al. (1999) and Nakariakov et al. (1999). After that the strong damping of coronal loop oscillations was confirmed by many observers (e.g. Aschwanden et al. (2002); Schrijver et al. (2002); Ofman and Aschwanden (2002)). The typical damping time of oscillations is a few oscillation periods. A few different mechanisms of damping were suggested (e.g. Roberts (2000)). Among them are the footpoint and side wave energy leakage, the phase mixing and the resonant absorption. Recently Morton and Erdélyi (2009) suggested that the observed rapid decrease in the oscillation amplitude can be caused be the loop cooling.

Simple estimates show that the damping due to the side wave energy leakage can cause the damping of coronal loop kink oscillations with the characteristic time at least by two orders of magnitude larger than the observed damping time (e.g. Ruderman (2005)). The situation with the footpoint leakage is not so clear. We do not know any accurate investigation of this damping mechanism.

The situation with the phase mixing is very strange. On one hand it was and remains a popular mechanism for explaining the damping of kink oscillations. On the other hand up to now there is no mathematical model of the damping of kink oscillations that incorporates this mechanism. From our point of view it is simply irrelevant.

As for the amplitude decrease due to the loop cooling, this is a very interesting suggestion, but it needs further investigation, so that we do not discuss it in this review.

At present the only damping mechanism that has a solid theoretical background is resonant absorption. It was suggested long ago by Hollweg and Yang (1988) that (that time hypothetical) kink oscillations of coronal magnetic loops can strongly damp due to resonant absorption.

After the kink oscillations of coronal magnetic loops were observed and the strong damping of these oscillations was reported, Ruderman and Roberts (2002) revived this old idea by Hollweg and Yang. As a model of a coronal magnetic loop they considered a cylindrical magnetic tube with the density homogeneous in the longitudinal direction but varying in a thin annulus at the tube boundary. This model is shown in Fig. 10. The background magnetic field has the constant magnitude and parallel to the z-axis of cylindrical coordinates r, φ, z. It is assumed that the thickness of the annulus, ℓ, is much smaller than the tube radius, $\ell \ll a$, and that the background density is given by

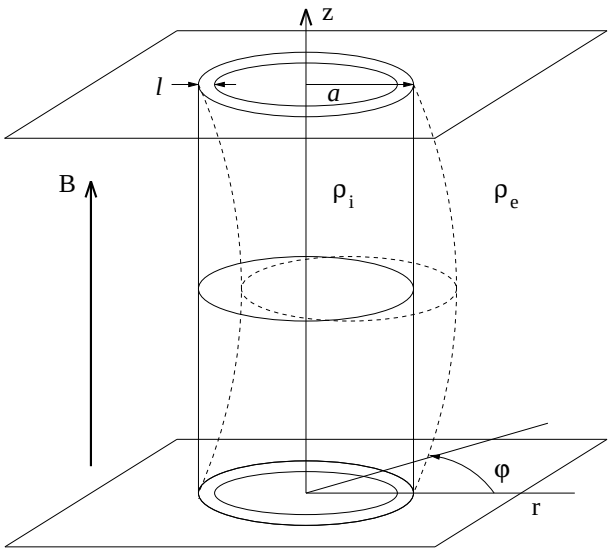

Fig. 10 A sketch of the equilibrium state, showing a magnetic flux tube with plasma density ρ_i embedded in a plasma with density ρ_e. The equilibrium magnetic field everywhere has strength B. The equilibrium density varies in the annulus region $a - \ell < r < a$ from ρ_i to ρ_e. The dashed lines show the perturbed magnetic tube in its kink mode of oscillation.

$$\rho(r) = \begin{cases} \rho_i, & r < a - \ell, \\ \dfrac{\rho_i}{2}\left[1 + \chi - (1-\chi)\sin\dfrac{\pi(2r + \ell - 2a)}{2\ell}\right], & a - \ell < r < a, \\ \rho_e, & r > a. \end{cases} \tag{58}$$

Here $\chi = \rho_e/\rho_i$. Ruderman and Roberts solved the initial value problem for the linearised MHD equations in the cold plasma approximation. They found that the kink

oscillation of the magnetic tube emerges from almost arbitrary perturbation in a few oscillation periods. Then it starts to damp due to resonant absorption of the wave energy in the vicinity of the resonant position inside the annulus. The resonant position is determined by the condition that, at this position, the frequency of the kink oscillation matches the local Alfvén frequency. In the thin tube thin boundary layer (TTTB) approximation they obtained that the ratio of the damping time to the oscillation period is given by

$$\frac{t_{\rm dec}}{P} = \frac{2a}{\pi\ell}\frac{\chi+1}{\chi-1}, \tag{59}$$

where $T = 2\pi/\omega_k$. This expression can be obtained as a particular case of a more general expression for the damping time given by Goossens et al. (1992). Substituting in equation (59) $T = 256$ s and $t_{\rm dec} = 870$ s reported by Nakariakov et al. (1999), Ruderman and Roberts found $\ell/a \approx 0.23$. Goossens et al. (2002) applied a similar analysis to estimate ℓ/a for a collection of loop oscillations using the data provided by Ofman and Aschwanden (2002). The results that they obtained are given in the table below:

Table 1.

No.	L [Mm]	a [Mm]	R/L	P [s]	$t_{\rm dec}$ [s]	ℓ/R
1	168	3.60	0.021	261	840	0.16
2	72	3.35	0.047	265	300	0.44
3	174	4.15	0.024	316	500	0.31
4	204	3.95	0.019	277	400	0.34
5	162	3.65	0.023	272	849	0.16
6	390	8.40	0.022	522	1200	0.22
7	258	3.50	0.014	435	600	0.36
8	168	3.15	0.019	143	200	0.35
9	406	4.60	0.011	423	800	0.26
10	192	3.45	0.018	185	200	0.46
11	146	7.90	0.054	396	400	0.49

In their paper Goossens et al. used the notation slightly different from that used by Ruderman and Roberts (2002). They denoted the loop radius as R, and the annulus containing the inhomogeneous plasma was defined by the inequality $R - \ell/2 < r < R + \ell/2$, so that $a = R + \ell/2$. In addition they used the linear density profile, so that the equilibrium density in their model was given by

$$\rho(r) = \begin{cases} \rho_i, & r < R - \ell/2, \\ \dfrac{\rho_i}{2}\left[1 + \chi + \dfrac{2}{\ell}(R-r)(1-\chi)\right], & R - \ell/2 < r < R + \ell/2, \\ \rho_e, & r > R + \ell/2. \end{cases} \tag{60}$$

For this density profile the ratio of the damping time and period is given by

$$\frac{t_{\rm dec}}{P} = \frac{4a}{\pi^2\ell}\frac{\chi+1}{\chi-1}. \tag{61}$$

If we use the sinusoidal density profile (58), then we obtain the values of ℓ/R approximately 1.57 times larger than those given in Table 1.

We can see that, at least for some events, the ratio ℓ/R is not small at all. This observation inspired Van Doorsselaere et al. (2004a) to study the damping of kink

oscillations of magnetic flux tubes numerically. The results of their numerical study are shown in Fig. 11 adopted from Van Doorsselaere et al. (2004a). This figure displays the results of the numerical calculations for a very thin tube, $R/L \approx 0.006$. However they remain practically the same for a much thicker tube with $R/L \approx 0.06$. We can see that even for the largest value of ℓ/R, which is $\ell/R = 0.49$, the difference between the values of $t_{\rm dec}/P$ obtained numerically and analytically in the TTTB approximation is less than 13%. Hence, we conclude that the analytic TTTB theory gives quite a reasonable approximation for the damping time.

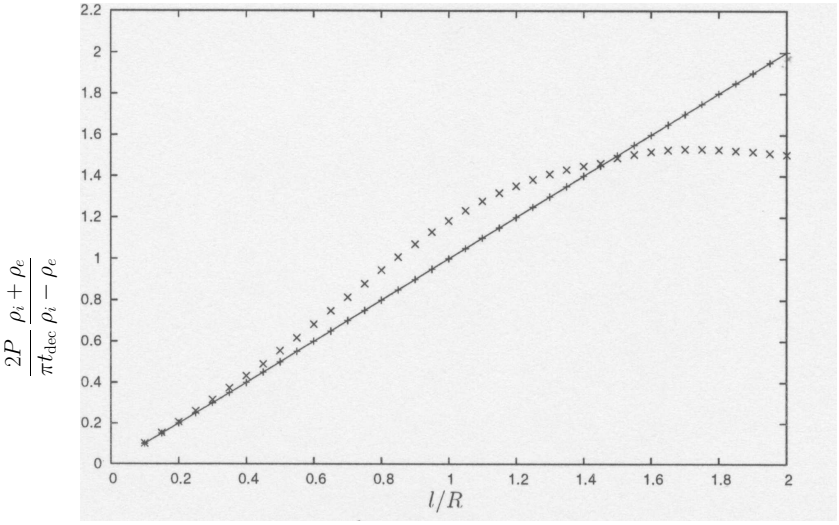

Fig. 11 The crosses show the numerically calculated ration of $P/t_{\rm dec}$, while the straight line gives this ratio calculated analytically with the use of the TTTB approximation. In this figure $R/L = 0.02/\pi \approx 0.006$ and $\chi = 0.1$.

Later the damping of kink oscillations of straight longitudinally stratified magnetic tubes due to resonant absorption was studied numerically by Andries et al. (2005b) in the TTTB approximation, and by Arregui et al. (2005, 2006) for the arbitrary thickness of the layer where the density varies in the radial direction. It was found that, qualitatively, the damping due to resonant absorption is the same in longitudinally stratified tubes and tubes homogeneous in the longitudinal direction. One interesting result found by Andries et al. (2005b) was that the longitudinal stratification practically does not affect the ratio $t_{\rm dec}/P$. Dymova and Ruderman (2006a) studied the damping of kink oscillations of straight longitudinally stratified magnetic tubes analytically with the use of the TTTB approximation. They rigorously proved that, if $\rho(r, z) = \rho_i(z)f(r)$, where $f(r) = 1$ for $r < a - \ell$, $f(r) = \chi$ for $r > a$, and $f(r)$ monotonically decreases for $a - \ell < r < a$, then the ratio $t_{\rm dec}/P$ is exactly the same as in the longitudinally homogeneous tube (i.e. in the tube with $\rho_i = {\rm const}$).

Terradas et al. (2006) studied numerically the resonant damping of kink oscillations of longitudinally stratified curved coronal loops and found that the curvature practically does not affect the damping. Recently Terradas et al. (2008) investigated the resonant damping of kink oscillations of longitudinally homogeneous coronal loops,

however with the density dependent on r and φ. They found that resonant absorption still provides quite efficient damping of kink oscillations.

The main conclusion that can be made on the basis of the numerous studies of resonant damping of kink oscillations is that resonant absorption is a very robust damping mechanism. The damping time due to resonant absorption is only weakly dependent on particular properties of the background state. A detailed review on resonant damping of coronal loop oscillations is given by Goossens et al. (2006).

11 Application to coronal seismology

Although the transverse coronal loop oscillation is an interesting phenomenon on its own, its main importance is related to its application to the coronal seismology. The idea of the coronal seismology was first put forward by Uchida (1970) and Roberts et al. (1984). This idea is similar to the idea of any seismology: to obtain information about a medium from the observations of the wave propagation in this medium. In the case of coronal seismology we would like to obtain information about the parameters of the coronal plasma and magnetic field from the observations of the MHD wave propagation in the solar corona. Recently it was suggested to consider coronal seismology as a part of magneto-seismology, which is the seismology based on observation of the propagation of MHD waves (Verth at al. (2007); **?**).

The observations of transverse coronal loop oscillations were first used for coronal seismology by Nakariakov and Ofman (2001). They used the event observed by TRACE on 14th July 1998 to estimate the magnetic field magnitude in a loop. In what follows we will briefly reproduce their analysis. On 14th July 1998 TRACE observed a transverse oscillation of a coronal loop with the length $L \approx 130$ Mm. The oscillation period was $T \approx 256$ s. The ion number density of the plasma in the loop was estimated to be $n_i \approx 1.6 \times 10^9$ cm^{-3}. The authors arbitrarily took $\rho_i/\rho_e = 10$, however this quantity only weakly affect the obtained results. For example, reducing this ratio to 3 changes the estimate of the magnetic field magnitude by less than 9%. Taking into account the uncertainty in the measurement of L, T and n_i this change is completely insignificant. The kink speed is given by $C_k = 2L/T \approx 1015$ km/s. Then the Alfvén speed in the loop is equal to $V_{Ai} = (1+\rho_e/\rho_i)^{1/2}(C_k/\sqrt{2}) \approx 752$ km/s, and we obtain the estimate for the magnetic field magnitude

$$B = V_{Ai}\sqrt{\mu_0 m_i n_i} \approx 13 \times 10^{-4} \text{ T} = 13\,(\pm 9) \text{ G}.$$

The error bar ± 9 is related with the uncertainty in the measurement of L, T and n_i. Hence, the final conclusion made by Nakariakov and Ofman (2001) was that the field magnitude should be between 4 and 22 Gauss. This estimate is in a good agreement with the estimates obtained by using other methods.

The second application of the observations of the transverse coronal loop oscillations to the coronal seismology is related to the estimate of atmospheric scale height in the corona. Verwichte et al. (2004) reported two cases of observations of the transverse coronal loop oscillations where, in addition to the fundamental harmonic, the first overtone was also observed. A very important property of these observations was that the ratio of the frequencies of the first overtone and the fundamental harmonic was less than 2. It was equal to 1.81 and 1.64 respectively (note that later Van Doorsselaere et al. (2007) used the improved technique to correct this values to 1.82 and 1.58). Andries et al. (2005a) suggested that this deviation of the frequency ratio from

2 is caused by the variation of the plasma density along the loop. Then they used this idea to obtain estimates for the coronal scale height. In their analysis they assumed that the corona is isothermal, and a coronal loop has the half-circle shape and situated in the vertical plane. In that case the radius of the half-circle, R, is related to the loop length L by $R = L/\pi$. If we introduce the coordinate along the loop, z, $0 \le z \le L$, and the height of a point in the loop in the solar atmosphere, h, then these two quantities are related by

$$h = \frac{L}{\pi} \sin \frac{\pi(L-z)}{L}.$$

In the isothermal atmosphere the plasma density in the loop is given by

$$\rho_i(z) = \rho_f e^{-h/H} = \rho_f \exp\left(-\frac{L}{\pi H} \sin \frac{\pi(L-z)}{L}\right),$$

where H is the atmospheric scale height and ρ_f is the density at the loop foot points. It was also assumed that the plasma temperature inside and outside the loop is the same, so that $\rho_i(z)/\rho_e(z) = \text{const}$. Then it was arbitrarily taken $\rho_i(z)/\rho_e(z) = 10$ (however once again the results are not very sensitive to this parameter). After that the frequencies of the fundamental harmonic and the first overtone were calculated, and their ratio was found as a function of H. It tunes out that this is a monotonically decreasing function. The inverse function gives H as a function of the ratio of frequencies of the fundamental harmonic and the first overtone. Using this technique Andries et al. (2005a) obtained that the atmospheric scale height was equal to 68 Mm in the first event, and 36 Mm in the second event.

Dymova and Ruderman (2006b) studied the effect of the loop shape on the estimate of the atmospheric scale height. They considered coronal loops with the shape of an arc of a circle of radius R immersed in an isothermal atmosphere. The loop shape is characterised by the parameter $\lambda = l/R$, where l is the distance from the circle centre to the the solar surface. This distance is considered as positive when the circle centre is below the solar surface and as negative when it is above. Then Dymova and Ruderman (2006b) fixed the height of the loop apex point, h_a, and obtained the estimates of H/h_a for λ varying from -0.9, which corresponds to an almost circular loop, to 0.9, which corresponds to an almost straight loop. They applied their analysis to the two cases of simultaneous observations of the fundamental mode and first overtone reported by Verwichte et al. (2004). As a result they obtained H varying from 79 to 59 Mm in the first case, and from 42 to 33 Mm in the second case. Recall that for loops with a half-circle shape Andries et al. (2005a) obtained the estimates for the atmospheric scale height equal to 68 Mm and 36 Mm respectively. We see that the loop shape is sufficiently important for the estimate of the atmospheric scale height.

Recently Ruderman et al. (2008) studied the effect of the loop expansion on the estimate of the atmospheric scale height. They showed that this estimate is a monotonically decreasing function of the loop expansion factor Γ, which is the ratio of the loop radius at the loop apex and the loop foot points. One illuminating example that they gave is the following. Van Doorsselaere et al. (2007) reported the third case of the simultaneous observation of the fundamental harmonic and the first overtone made by TRACE in 1998. Using the technique developed by Andries et al. (2005a) and assuming that the radius of the loop cross-section does not vary along the loop they obtained the estimate for the atmospheric scale height 109 Mm. It is about twice larger than the scale height calculated on the basis of the measurement of the temperature. Van Doorsselaere et al. (2007) interpreted their result as the evidence that the observed

loop was not in the equilibrium. Not claiming that this interpretation is wrong Ruderman et al. (2008) suggested another possible interpretation. If we assume that the loop expansion factor is $\Gamma = 1.5$, then we obtain the estimate $H \approx 50$ Mm, which is in a complete agreement with the estimate of H calculated on the basis of the measurement of the temperature for the loop in equilibrium.

A more detailed discussion of the use of simultaneous observations of the fundamental harmonic and overtones of the kink oscillations of coronal loops for coronal seismology is given by Andries et al. (2009).

12 Discussion and conclusions

We see that a very serious progress in the theory of the transverse coronal loop oscillations was made in the decade that passed after the first observation of this oscillations made by TRACE in 1998. The new more sophisticated models of this phenomenon incorporating such effects as the density and cross-section radius variation along the loop, the loop curvature, the loop non-circular cross-section, and the magnetic twist were developed. The resonant absorption was identified as the most probable mechanism of the oscillation damping. The theoretical basis for the application of observations of coronal loop transverse oscillations to coronal seismology was created.

The method of asymptotic expansions was proved to be a powerful tool for studying the transverse coronal loop oscillations. Its applicability is based on the fact that the observed coronal loops are thin structures. The results obtained with the use of this method are practically the same as those obtained with the use of sophisticated numerical studies. A substantial progress was made in studying the resonant damping of the transverse oscillation with the aid of the TTTB (thin tube thin boundary layer) approximation. However the accuracy of the thin boundary layer approximation, in general, is much lower than that of the thin tube approximation, so that parallel numerical study of damping is desirable.

In spite of all achievements of the theory of transverse coronal loop oscillations it is still very far from its completion. There are large number of outstanding problems that are a real challenge to theorists. In what follows we try to present a list of these unsolved problems. The reader should keep in mind that this list is very far from being complete.

An important problem in application to the coronal seismology is the robustness of models that we use. Up to now in the majority of models describing the transverse oscillations of coronal loops it is assumed that the loop cross-section is circular. However, at present there are no observational evidences supporting this assumption. Hence, it is very important to find out how much the eigenfrequencies and eigenmodes of the fast kink oscillations of magnetic tubes depend on the shape of the cross-section. The first step in this direction was made by Ruderman (2003) and Erdélyi and Morton (2009) who studied the oscillations of tubes with the elliptic cross-section. But it is desirable to study the fast kink oscillations of tubes with arbitrary cross-sections.

At present only oscillations of plane loops, i.e. loops with axes that are planar curves were studied. However there are observation evidences that at least some of loops are not plane and their axes are three-dimensional curves with the non-zero torsion. The effect of torsion on the fast kink oscillations of magnetic tubes should be studied.

The effect of loop cooling on fast kink oscillations of coronal loops deserves serious attention. The first step in studying this problem has been made by Morton and Erdélyi

(2009) who used the simplest possible model of a cooling loop. Studying this effect using more realistic models for the description of non-stationary background states of cooling loops is on the agenda.

In accordance with the observations very often the displacement of the loop axis is of the order of or even larger than the radius of the loop cross-section. In that case the linear description of fast kink oscillations is not valid anymore and nonlinear effects should be taken into account. The development of the nonlinear theory of fast kink oscillations of coronal loops is, from our point of view, the most challenging problem for theorists studying the transverse oscillations of coronal loops.

Acknowledgements MR and RE acknowledge the financial support from the Science and Technology Facilities Council (STFC), UK. RE is thankful to M. Kéray for patient encouragement and is also grateful to NSF, Hungary (OTKA, Ref. No. K67746).

References

J. Andries, I. Arregui, M. Goossens, Astrophys. J, **624**, L57 (2005a)
J. Andries, M. Goossens, J.V. Hollweg, I. Arregui, T. Van Doorsselaere, Astron. Astrophys., **430**, 1109 (2005b)
J. Andries, E. Verwichte, B. Roberts, T. Van Doorsselaere, G. Verth, R. Erdélyi, this issue (2009)
I. Arregui, T. Van Doorsselaere, J. Andries, M. Goossens, D. Kimpe, **441**, 361 (2005)
I. Arregui, T. Van Doorsselaere, J. Andries, M. Goossens, D. Kimpe, Phil. Trans. R. Soc. A, **364**, 529 (2006)
M.J. Aschwanden, Phil. Trans. Roy. Soc. A, **364**, 417 (2006)
M.J. Aschwanden, B. De Pontieu, C.J. Schrijver, A.M. Tilte, Solar Phys., **206**, 99 (2002)
M.J. Aschwanden, L. Fletcher, C.J. Schrijver, D. Alexander, Astrophys. J., **520**, 880 (1999)
M.J. Aschwanden, R.W. Nightingale, D. Alexander, Astrophys. J., **541**, 1059 (2000)
K. Bennett, B. Roberts, U. Narain, Solar Phys., **185**, 41 (1999)
B.K. Carter, R. Erdélyi, Astron. Astrophys., **475**, 323 (2007)
B.K. Carter, R. Erdélyi, Astron. Astrophys., **481**, 239 (2008)
M.V. Dymova, M.S. Ruderman, Solar Phys., **229**, 79 (2005)
M.V. Dymova, M.S. Ruderman, Astron. Astrophys., **457**, 1059 (2006a)
M.V. Dymova, M.S. Ruderman, Astron. Astrophys., **459**, 241 (2006b)
P.M. Edwin, B. Roberts, Solar Phys., **88**, 179 (1983)
R. Erdélyi, in *Physics of the Sun and its Atmosphere*, B.N. Dwivedi, U. Narain (eds.), World Scientific, Singapore, pp. 61–108 (2008)
R. Erdélyi, B.K. Carter, Astron. Astrophys., **455**, 361 (2006)
R. Erdélyi, V. Fedun, Solar Phys., **238**, 41 (2006)
R. Erdélyi, V. Fedun, Solar Phys., **246**, 101 (2007)
R. Erdélyi, R. Morton, Astron. Astrophys., **494**, 269 (2009)
M. Goossens, J. Andries, I. Arregui, Phil. Trans. R. Soc. A, **364**, 433 (2006)
M. Goossens, J. Andries, M.J. Aschwanden, Astron. Astrophys., **394**, L39 (2002)
M. Goossens, J.V. Hollweg, T. Sakurai, Solar Phys., **138**, 233 (1992)
J.V. Hollweg, G. Yang, J. Geophys. Res., **93**, 5423 (1988)
D.B. Jess, M. Mathioudakis, R. Erdélyi, P.J. Crockett, F.P. Keenan, D.J. Christian, Science, in press (2009)
M. Luna, J. Terradas, R. Oliver, J.L. Ballester, Astrophys. J., **676**, 717 (2008)
B.B. Mikhalyaev, A.A. Solov'ev, A.A., Solar Phys., **227**, 249 (2005)
R. Morton, R. Erdélyi, Astrophys. J., submitted (2009)
V.M. Nakariakov, L. Ofman, Astron. Astrophys., **372**, L53 (2001)
V.M. Nakariakov, L. Ofman, E.E. DeLuca, B. Roberts, J.M. Davila, Science, **285**, 862 (1999)
V.M. Nakariakov, E. Verwichte, Living Rev. Solar Phys., **2**, 3 (2005)
L. Ofman, M.J. Aschwanden, Astrophys. J., **576**, L153 (2002)
E. Robbrecht, E. Verwichte, D. Berghmans, J.F. Hochedez, S. Poedts, V.M. Nakariakov, Astron. Astrophys., **370**, 591 (2001)

B. Roberts, Solar Phys., **69**, 39 (1981)
B. Roberts, Solar Phys., **193**, 139 (2000)
B. Roberts, P.M. Edwin, A.O. Benz, Astrophys. J., **279**, 857 (1984)
B. Roberts, V.M. Nakariakov, in *Turbulence, Waves and Instabilities in the Solar Plasma*, R. Erdélyi, K. Petrovay, B. Roberts, M. Aschwanden (eds.) , *NATO Sciences Series*, Vol. 124, Kluwer, pp. 239–274 (2003)
M.S. Ruderman, Astron. Astrophys., **409**, 287 (2003)
M.S. Ruderman, ESA SP-600 (2005)
M.S. Ruderman, Solar Phys., **246**, 119 (2007)
M.S. Ruderman, B. Roberts, Astrophys. J., **577**, 475 (2002)
M.S. Ruderman, G. Verth, R. Erdélyi, Astrophys. J., **686**, 694 (2008)
D.D. Ryutov, M.P. Ryutova, Sov. Phys.—JETP, **43**, 491 (1976)
C.J. Schrijver, M.J. Aschwanden, A.M. Tilte, Solar Phys., **206**, 69 (2002)
C.J. Schrijver, D.S. Brown, Astrophys. J., **537**, L69 (2000)
J. Terradas, this issue (2009)
J. Terradas, I. Arregui, R. Oliver, J.L. Ballester, J. Andries, M. Goossens, Astrophys. J., **679**, 1611 (2008)
J. Terradas, R. Oliver, J.L. Ballester, Astrophys. J., **650**, L91 (2006)
Y. Uchida, Publ. Astron. Soc. Japen, **22**, 341 (1970)
T. Van Doorsselaere, J. Andries, S. Poedts, M. Goossens, Astrophys. J., **606**, 1223 (2004a)
T. Van Doorsselaere, A. Debosscher, J. Andries, S. Poedts, Astron. Astrophys., **424**, 1065 (2004b)
T. Van Doorsselaere, V.M. Nakariakov, E. Verwichte, Astron. Astrophys., **473**, 959 (2007)
T. Van Doorsselaere, M.S. Ruderman, D. Robertson, Astron. Astrophys., **485**, 849 (2008)
T. Van Doorsselaere, E. Verwichte, J. Terradas, this issue (2009)
G. Verth, R. Erdélyi, Astron. Astrophys., **486**, 1015 (2008)
G. Verth, R. Erdélyi, Astrophys. J., **687**, L45 (2008)
G. Verth, T. Van Doorsselaere, R. Erdélyi, M. Goossens, Astron. Astrophys., **475**, 341 (2007)
E. Verwichte, V.M. Nakariakov, L. Ofman, E.E. Deluca, Solar Phys., **223**, 77 (2004)
T.J. Wang, S.K. Solanki, Astron. Astrophys., **421**, L33 (2004)
T.J. Wang, S.K. Solanki, M. Selwa, Astron. Astrophys., **489**, 1307 (2008)
Y.D. Zhugzhda, M. Goossens, Astron. Astrophys., **377**, 330 (2001)